J Biol Phys (2011) 37:39–50
DOI 10.1007/s10867-010-9194-4

ORIGINAL PAPER

Biological cell–electrical field interaction: stochastic approach

A. K. Dubey · M. Banerjee · Bikramjit Basu

Received: 7 February 2010 / Accepted: 12 July 2010 /
Published online: 17 August 2010

Abstract The present work demonstrates how a stochastic model can be implemented to obtain a realistic description of the interaction of a biological cell with an external electric field. In our model formulation, the stochasticity is adopted by introducing various levels of forcing intensities in model parameters. The presence of noise in nuclear membrane capacitance has the most significant effect on the current flow through a biological cell. A plausible explanation based on underlying physics and biological structure of the nuclear membrane is proposed to explain such results.

Keywords Biological cell · Micro-organelles · E-field · Stochasticity

1 Introduction

In recent years, considerable interest has been generated in investigating the influence of electric field on various biophysical and biochemical processes in laboratory scale experiments and in clinical trials [1–5]. In this context, the influence of pulsed electric fields, in contrast to continuous electric fields of similar characteristics, is reported to be significant [6]. For example, low frequency pulsed electric fields could stimulate bone growth and accelerate fracture healing [7]. Also, the effect of the electric field depends upon its pulse duration, field strength and cell type. In addition, short pulses of electric fields can induce electroporation, a rapid structural rearrangement of the membrane with the formation

A. K. Dubey · B. Basu (✉)
Laboratory for Biomaterials, Department of Materials and Metallurgical Engineering,
Indian Institute of Technology, Kanpur, India
e-mail: bikram@iitk.ac.in

M. Banerjee
Department of Mathematics and Statistics,
Indian Institute of Technology, Kanpur, India

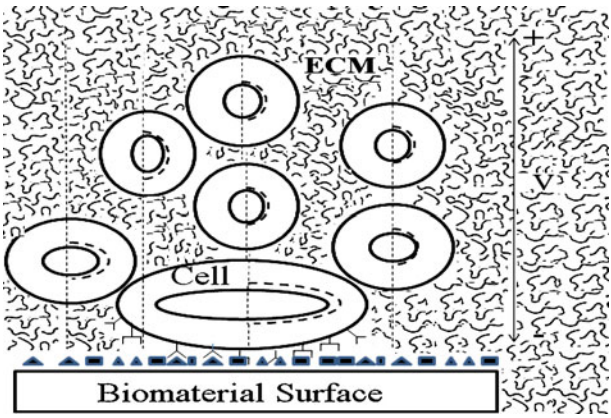

Fig. 1 Schematic of the macroscopic view of the passage of electrical current through multiple cells, dispersed in extracellular matrix (ECM)

of transient pores [8]. As a consequence, the transport of ions across the membrane and hence, the current density changes abruptly. A dynamic interaction of cells with electric field involving both the membrane charging and discharging governs the rapid increase in membrane conductivity and consequently, the pore formation dynamics [8]. It has a number of applications in gene therapy, transdermal drug delivery and bacterial decontamination [3]. In a recent work [9], we reported a deterministic model to analytically evaluate the time constant for the electrical analog of near spherical shaped biological cells. The presence of various cellular organelles as well as dynamic changes in cell size during the cellular adaptation process was not considered in our earlier work. Each cellular organelle has a distinctly different structure and chemical constituents. As a result, resistances offered by each of these would be different and rigorous use of any deterministic model is to be made to capture the overall response of all the cellular organelles. Also, cells change their size dynamically either as a result of the response to an external field (E-field) or in contact with a biomaterial surface [9, 10] (see Fig. 1). Therefore, randomness or stochasticity must play an important role in response of any biological system to an E-field. In above perspective, the objective of the present paper is to develop a stochastic model of a non-linear cell-electric field system under random perturbation. It is reported in the literature that a stochastic model provides a more realistic description of a biological system than its deterministic counterpart [11–14].

2 Basic model

In our earlier work [9], the deterministic model to understand the interaction of electric field with a single living cell was developed by considering the hypothesis of an electric analog of cells (Fig. 2). The analysis of electric equivalent circuit of a cell leading to a solution of time constant is based upon a set of assumptions, which hold true for the present work.

Referring to Fig. 2, let C_S and R_S denote the capacitance and resistance of the extracellular matrix, C_m and C_n stand for the capacitance of the cell and nuclear membrane, R_{C_1}, R_{C_2} and R_{C_3} are resistances of cytoplasm, depending on spatial region, respectively, and R_n

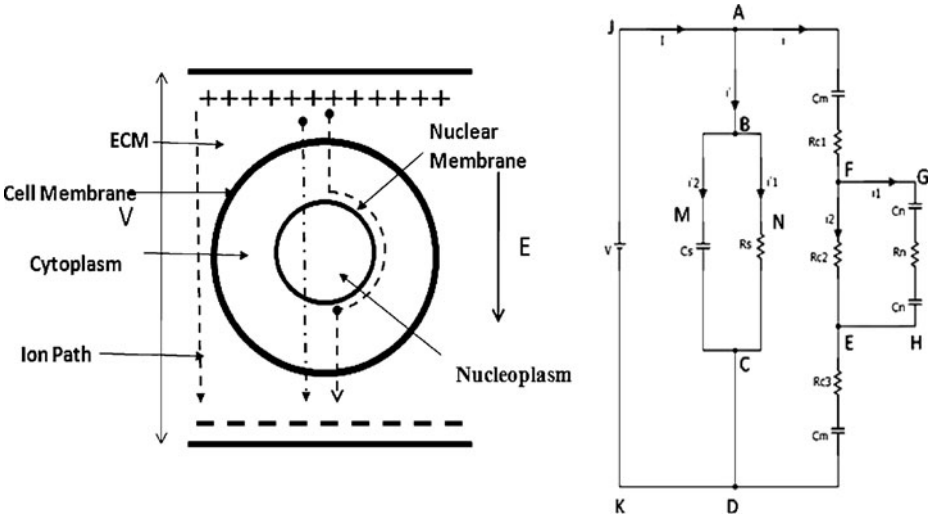

Fig. 2 The electrical analog circuit of a single cell, placed in an electric field

is the resistance of nucleoplasm. Applying Kirchhoff's laws at various nodes of Fig. 2 and the first principle analysis for various circuit components at nodes *A*, *B* and *F* leads us to obtain,

$$I = i + i' \tag{1}$$

$$i' = i'_1 + i'_2 \tag{2}$$

$$i = i_1 + i_2 \tag{3}$$

Applying Kirchhoff's voltage law for the loop *EFGHE*, we obtain

$$i_2(t) = \zeta i_1(t) + \eta \int_0^t i_1(s)\mathrm{d}s \tag{4}$$

where $\zeta = R_n/R_{C_2}$ and $\eta = 2/R_{C_2}C_n$. Adopting a similar approach for the loop *JAFEDKJ*, one can obtain

$$V = \frac{2}{C_m}\int_0^t i(s)\mathrm{d}s + \left(R_{C_1} + R_{C_3}\right) i(t) + R_{C_2} i_2(t). \tag{5}$$

Differentiating (5) and then eliminating i_2 with help of (3) and (4), we obtain

$$a\frac{di_1(t)}{dt} + bi_1(t) + c\int_0^t i_1(s)\mathrm{d}s = 0 \tag{6}$$

Table 1 Resistance and capacitance values for various cell sizes

Parameters	Cell radius (15 μm)	Cell radius (25 μm)
R_{C_1} (KΩ)	55.7	33.49
R_{C_2} (KΩ)	25	14.8
R_{C_3} (KΩ)	55.7	33.49
R_n (KΩ)	286.56	173.34
C_n (F)	6.098×10^{-12}	1.694×10^{-11}
C_m (F)	2.826×10^{-11}	7.85×10^{-11}

where

$$a = \frac{\left(R_{C_1} + R_{C_2} + R_{C_3}\right) R_n + R_{C_2}\left(R_{C_1} + R_{C_2}\right)}{R_{C_2}}$$

$$b = \frac{2}{C_m} + \frac{2R_n}{R_{C_2} C_m} + \frac{2\left(R_{C_1} + R_{C_2} + R_{C_3}\right)}{R_{C_2} C_n}, \quad c = \frac{4}{C_m C_n R_{C_2}}.$$

Further differentiating (6), we get

$$\frac{d^2 i_1(t)}{dt^2} + \alpha \frac{d i_1(t)}{dt} + \beta i_1(t) = 0 \tag{7}$$

where $\alpha = b/a$ and $\beta = c/a$. Solving (7), we get $i_1(t)$, and then substituting in (4), we can obtain $i_2(t)$. Using the expressions for $i_1(t)$ and $i_2(t)$, we get $i(t)$ (see (3)).

We selected the noise parameters, assuming that the cells change their size (radius) between 15 to 25 μm during cell–E-field interaction. Such change in size of eukaryotic cells are consistent with literature reports [10]. Following the geometrical approaches, as outlined in [9], the calculated values of resistances and capacitances for the selected cell sizes are summarized in Table 1.

Using the values of Table 1, one can obtain $\alpha = 1.627 \times 10^6$, $\beta = 5.656 \times 10^{11}$, $\zeta = 11.4624$ and $\eta = 1{,}315{,}789$ for a cell of radius 15 μm and $\alpha = 9.836 \times 10^5$, $\beta = 2.061 \times 10^{11}$, $\zeta = 11.71216$ and $\eta = 8{,}140{,}671$ for a cell with radius 25 μm, respectively (for convenience, the units for the parameters not given). Thus, we can say that if the cell radius varies within the range of 15–25 μm, then $\alpha \in \left[9.836 \times 10^5, 1.627 \times 10^6\right]$ and $\beta \in \left[2.0615 \times 10^{11}, 5.656 \times 10^{11}\right]$. As the cell size does not remain constant during cell–E-field interaction, one can assume that the capacitances as well as resistances are not fixed quantities at all times t. In order to incorporate this idea into our modelling approach, we can extend (7) to a stochastic differential equation (SDE) model by incorporating white noise terms into the coefficients (α, β) involved in (7). In the next section, we will consider the SDE model corresponding to the deterministic models and describe a possible way to solve the resulting equations.

3 Stochastic differential equation model

The aim of this section is to analyze the effects of white noise perturbation on the system parameters. Formally, a white noise process is the pathwise derivative of the Wiener process [15, 16]. For this purpose, we can consider α and β as system parameters and we perturb the parameters, α and β by incorporating white noise terms as follows,

$$\alpha = \alpha_0 + \sigma_1 \xi_1(t), \quad \beta = \beta_0 + \sigma_2 \xi_2(t)$$

where α_0 and β_0 are mid-points of the intervals $I_\alpha \equiv [983{,}610.33,\ 1{,}627{,}246.34]$ and $I_\beta \equiv [206{,}145{,}945{,}384.29,\ 565{,}565{,}473{,}565.01]$, respectively; $\xi_1(t)$ and $\xi_2(t)$ are two independent Gaussian white noise terms characterized by $\langle \xi_1(t) \rangle = \langle \xi_2(t) \rangle = 0$ and $\langle \xi_i(t)\xi_j(s) \rangle = \delta_{ij}\delta(t-s)$, $(i, j = 1, 2)$ and σ_1, σ_2 (> 0) are the noise intensities; δ is the Dirac-delta function, δ_{ij} is the Kronecker delta and $\langle . \rangle$ stands for ensemble average. We have to choose the magnitude of σ_1 and σ_2 in such a way that α and β are likely to be within I_α and I_β respectively. These restrictions have been subsequently considered during numerical simulation. As a first step towards stochastic modeling of cell–electric field interaction, we assume that the noise terms are uncorrelated. The stochastic analog to the deterministic (7) is,

$$\frac{d^2 i_1(t)}{dt^2} + (\alpha_0 + \sigma_1 \xi_1(t)) \frac{di_1(t)}{dt} + (\beta_0 + \sigma_2 \xi_2(t)) i_1(t) = 0. \tag{8}$$

Writing $x_1(t) = i_1(t)$ and $x_2(t) = \dfrac{di_1}{dt}$, (8) can be written as

$$dX(t) = f(X(t))dt + g(X(t))dW(t) \tag{9}$$

where $X(t) = [x_1(t),\ x_2(t)]^T$, $W(t) = [w_1(t),\ w_2(t)]^T$,

$$f(X(t)) = \begin{bmatrix} x_2(t) \\ -\beta_0 x_1(t) - \alpha_0 x_2(t) \end{bmatrix}, \quad g(X(t)) = \begin{bmatrix} 0 & 0 \\ -\sigma_2 x_1(t) & -\sigma_1 x_2(t) \end{bmatrix},$$

and $dw_i(t) = \xi_i(t)dt$, $i = 1,\ 2$. The solution of stochastic differential system with $X(t_0) = X_0$ is an Ito process [17–20]. Our next task is to solve the following system of equations by the multi-dimensional Euler–Maruyama (EM) method [21],

$$dX(t) = f(X(t))dt + g(X(t))dW(t), \quad X(t_0) = X_0, \quad t \in [t_0,\ T]. \tag{10}$$

Considering the discretization of the time interval $[0,\ T]$,

$$0 = t_0 < t_1 < t_2 < t_3 < \cdots < t_N = T,$$

the numerical solutions for $x_1(t)$ and $x_2(t)$ are given by

$$X^k_{n+1} = X^k_n + f^k(X^1_n, X^2_n)\Delta_{t_n} + g_{k1}(X^1_n, X^2_n)\Delta W^1_n + g_{k2}(X^1_n, X^2_n)\Delta W^2_n, \quad k = 1,\ 2 \tag{11}$$

with $X_0 \equiv (X^1_0,\ X^2_0)$ and $n = 0,\ 1,\ 2,\ \cdots,\ N-1$. In (11), $\Delta_{t_n} = t_{n+1} - t_n$ and $\Delta W^k_n = W^k(t_{n+1}) - W^k(t_n)$ for $n = 0,\ 1,\ 2,\ \cdots,\ N-1$ with $W^k(t_0) = 0$. The noise increments are $N(0,\ \Delta_{t_n})$-distributed independent random variables. The numerical solution $X^1_n \equiv X^1(t_n)$ gives $i_1(t)$ at $t = t_0, t_1, \cdots, t_n$.

Due to variation of cell sizes, the quantities R_n, R_{C_2} and C_n fluctuate within some finite interval, as determined by changes of cell size. The current $i_2(t)$ can be obtained from the following equation with the help of numerically simulated values of $i_1(t)$. The governing equation for $i_2(t)$ is

$$i_2(t) = (\zeta_0 + \sigma_3 \xi_3(t)) i_1(t) + (\eta_0 + \sigma_4 \xi_4(t)) \int_0^t i_1(s)\mathrm{d}s \tag{12}$$

where $\xi_3(t)$ and $\xi_4(t)$ have the meaning mentioned earlier and we choose σ_3 and σ_4 in such a way that $11.46 \le \zeta_0 + \sigma_3 \xi_1(t) \le 11.71$ and $1{,}315{,}789 \le \eta_0 + \sigma_4 \xi_2(t) \le 8{,}140{,}671$. Taking $\zeta_0 = 11.58$, $\eta_0 = 4{,}728{,}230$ and using the values $i_1(t_n)$, we get $i_2(t_n)$ using the numerical scheme

$$i_2(t_n) = (\zeta_0 + \sigma_3 \xi_1(t_n)) i_1(t_n) + (\eta_0 + \sigma_4 \xi_2(t_n)) \int_0^{t_n} i_1(s)\mathrm{d}s. \tag{13}$$

In order to compare the deterministic results with their stochastic counterparts, we have numerically simulated the values of $i_1(t)$ and $i_2(t)$. Consequently, the total current is computed.

4 Simulation results and discussion

For the deterministic model, (4) and (7) were solved numerically to get the steady state value of $i(t)$ and plotted in Fig. 3a. For the stochastic model, the time evolution of $i_1(t)$ and $i_2(t)$ were simulated using the numerical scheme as described in (11) and (13), respectively. The simulation results were used to obtain $i(t)$ for different forcing intensities (for fixed $\sigma_1 = 6.43 \times 10^4$, $\sigma_2 = 3.59 \times 10^{10}$ and three different sets of values for σ_3 and σ_4; (1) $\sigma_3 = 0.025$, $\sigma_4 = 6.82 \times 10^5$, (2) $\sigma_3 = 0.015$, $\sigma_4 = 3.82 \times 10^5$, (3) $\sigma_3 = 0.005$, $\sigma_4 = 5.82 \times 10^4$. Figure 3b–d depict the fluctuation of $i(t)$ around the steady state value and the amplitude of the oscillation depends upon the forcing intensities. Qualitatively, the trend of the variation in $i(t)$ with time is similar, except for the presence of significant noise around the steady-state values obtained using deterministic model. In particular, as the forcing intensities decrease, the bandwidth of fluctuation in $i(t)$ also decreases. It can be mentioned here that the assumption of cytoplasm and nucleoplasm as homogeneous media provides the deterministic values of $i(t)$. However, the presence of a number of micro-organelles in the

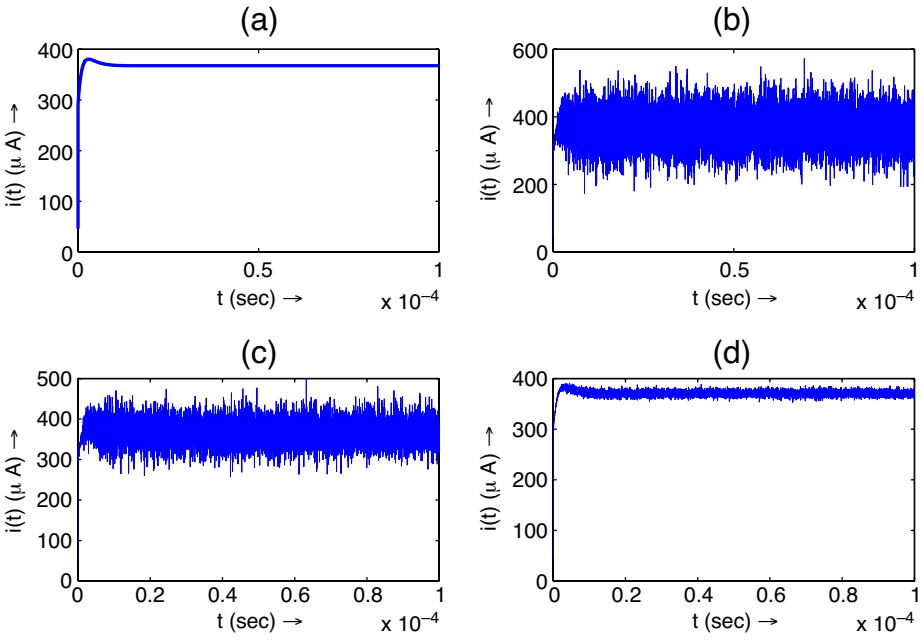

Fig. 3 Plot of $i(t)$ against time for fixed $\sigma_1 = 6.43 \times 10^4$, $\sigma_2 = 3.59 \times 10^{10}$ and different forcing intensities for σ_3 and σ_4, **b** $\sigma_3 = 0.025$, $\sigma_4 = 6.82 \times 10^5$, **c** $\sigma_3 = 0.015$, $\sigma_4 = 3.82 \times 10^5$, **d** $\sigma_3 = 0.005$, $\sigma_4 = 5.82 \times 10^4$. For comparison, the deterministic values of $i(t)$ are plotted in **a**

cytoplasm is responsible for the numerically observed fluctuations of the passage time of current through a living cell. In addition to various organelles, the cytosol contains various ions, small as well as large biological molecules. Depending on local pH or side groups in the amino acid sequence, various protein molecules exist in a charged state. The presence of an E-field also contributes to the fluctuations of such charged ions/molecules. Therefore, the combined influence of the organelles as well as aperiodic motion of charged biomolecules can explain the observed fluctuation over steady-state $i(t)$ values.

We have made an attempt to capture this idea with the help of the formulation of stochastic model systems, based upon the deterministic counterpart [9]. Due to stochastic considerations of the model system, the time constant is no longer a fixed value. In this case, we define the time constant as the time required to reach 62.3% of the average steady state values of $i(t)$. In reality, the position of the cellular organelles as well as the number of some specific organelles like mitochondria do not remain fixed. Hence, a fluctuation in time constant is anticipated. Therefore, in order to verify whether the time needed by $i(t)$ to reach the time constant value varies, four numerical runs following (13) were carried out, for the forcing intensities, $\sigma_1 = 6.43 \times 10^4$, $\sigma_2 = 3.59 \times 10^{10}$, $\sigma_3 = 0.025$, $\sigma_4 = 6.82 \times 10^5$. It is clear from the results presented in Fig. 4a–d that the time needed to reach the time constant is not a fixed value. In fact, $i(t)$ reaches the time constant value at $t = 1 \times 10^{-6}$s (approx.) during the first runs. However, $i(t)$ reaches the same time constant value in less than 1×10^{-6} s in two other runs. The above variation in timescale with numerical run essentially reflects our initial hypothesis that cell–electric field interactions are stochastic in nature.

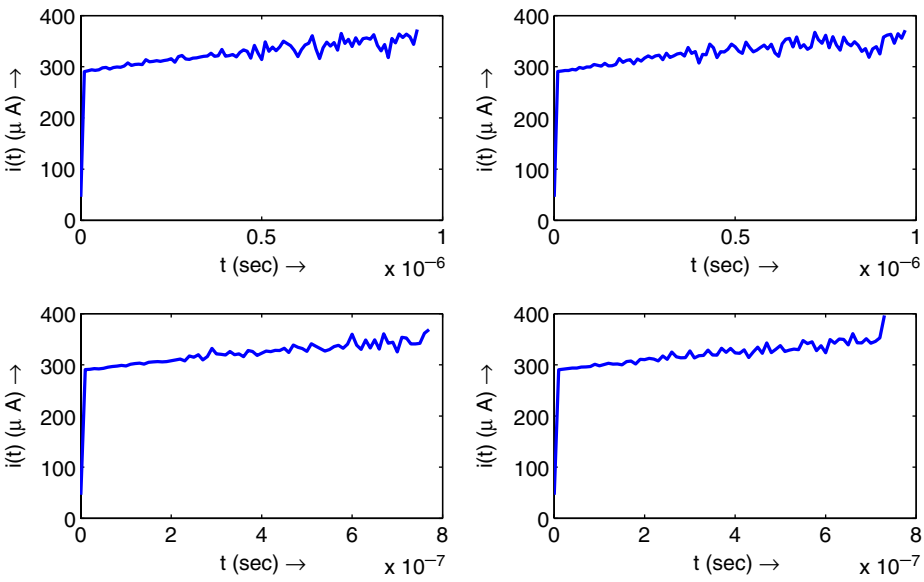

Fig. 4 Plot of $i(t)$ before reaching the time constant values for four different numerical runs with forcing intensities $\sigma_1 = 6.43 \times 10^4$, $\sigma_2 = 3.59 \times 10^{10}$, $\sigma_3 = 0.025$, $\sigma_4 = 6.82 \times 10^5$

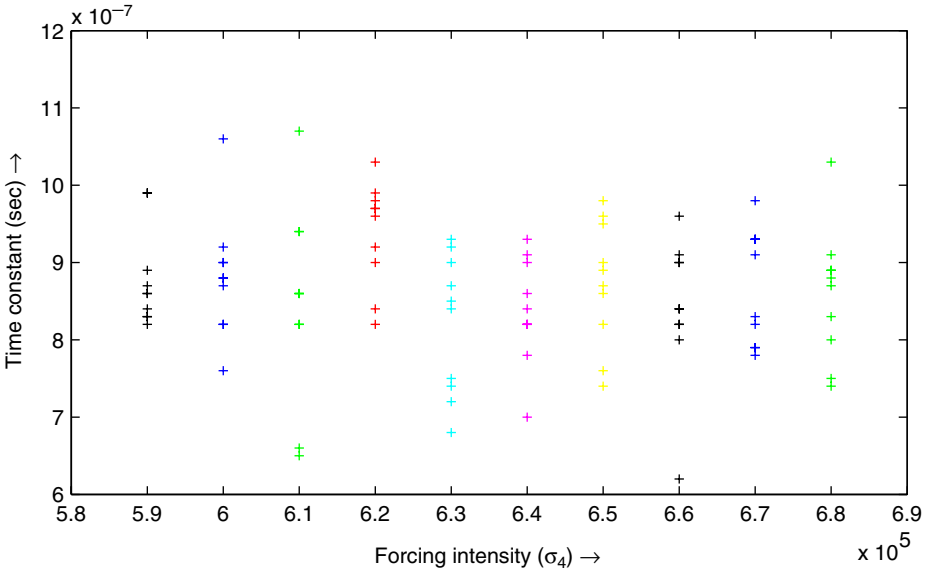

Fig. 5 Plot of time constant for stochastic case at different forcing intensities on η (for different values of σ_4 as mentioned in the scale of horizontal axis). Numerical simulations are performed for the parametric values $\alpha_0 = 1.305 \times 10^6$, $\beta_0 = 3.858 \times 10^{11}$, $\zeta_0 = 11.58$, $\eta_0 = 4728230$ and fixed forcing intensities $\sigma_1 = 6.43 \times 10^4$, $\sigma_2 = 3.59 \times 10^{10}$ and $\sigma_3 = 0.025$

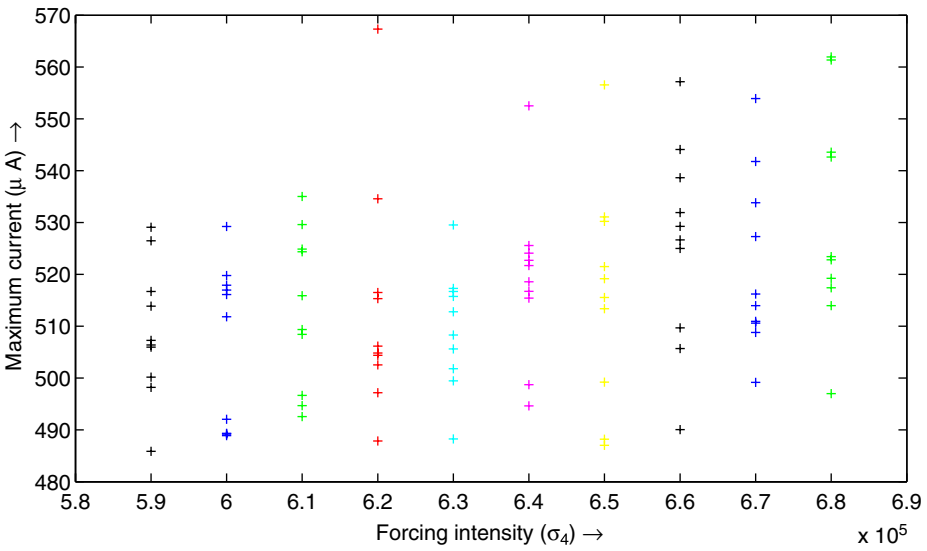

Fig. 6 Plot of maximum values attained by $i(t)$ at different forcing intensities σ_4, and all other parameter values are same as mentioned in the caption of Fig. 5

A question naturally arises: what will be the effect of changing intensities on the values of the time constant? Figure 5 depicts the calculated time constant for different forcing intensities on η and for ten trial runs for a particular value of the intensity. It can be reiterated here that the variation of cell size over 15 μm to 25 μm will yield different values of R_{C_1}, R_{C_2}, R_{C_3}, C_m, C_n and R_n. Instead of giving perturbations to individual resistance/capacitance values, we have perturbed the terms α, β, η and ζ such that they will lie in the estimated interval. From numerical simulations, it was revealed that C_n should have a significant impact on the time evolution of $i_2(t)$ and in turn on $i(t)$. It was also evident from the fact that the η term contains C_n in the denominator (magnitude of the order of 10^{-12}). To incorporate this idea, we have performed numerical simulations by perturbing α, β and ζ with fixed intensities $\sigma_1 = 6.43 \times 10^4$, $\sigma_2 = 3.59 \times 10^{10}$ and $\sigma_3 = 0.025$ and different forcing intensities σ_4 starting from 5.9×10^5 to 6.8×10^5. In Figs. 6 and 7, the max. and min. values of $i(t)$ are plotted against the forcing intensity σ_4. From the plotted data in Figs. 6 and 7, it is clear that the width of stochastic fluctuation increases gradually with an increase in magnitude of forcing intensities on η. Finally, the calculated values of the time constant are plotted against the increasing intensity of fluctuation in η in Fig. 5. Although the magnitude of the time constant fluctuates, one can easily verify that its average lies within a small interval with center at the deterministic value of the time constant. In Figs. 8 and 9, the mean and standard deviation of $i(t)$, obtained from 100 simulation runs of (8) and (12) for the parametric values $\alpha_0 = 1.305 \times 10^6$, $\beta_0 = 3.858 \times 10^{11}$, $\zeta_0 = 11.58$, $\eta_0 = 4728230$ and intensity of fluctuations $\sigma_1 = 6.43 \times 10^4$, $\sigma_2 = 3.59 \times 10^{10}$, $\sigma_3 = 0.015$ and $\sigma_4 = 3.82 \times 10^5$ are plotted. The mean of $i(t)$ at any time t fluctuates around the deterministic steady-state values for $i(t)$. The plot for standard deviation shows significant fluctuation around the mean value, which is quite expected for cell–electric field interaction.

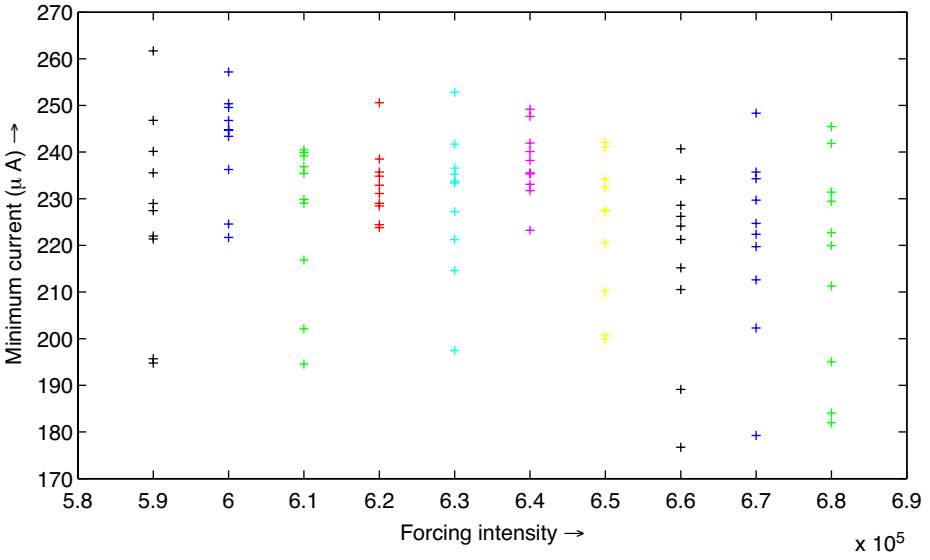

Fig. 7 Plot of minimum values attained by $i(t)$ at different forcing intensities σ_4, these minimum values are obtained from the numerical simulations carried out for Fig. 6

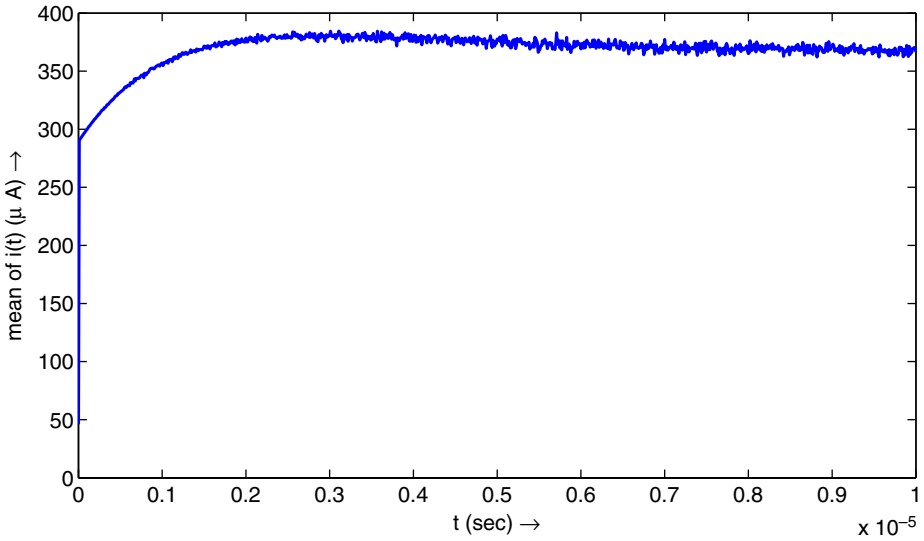

Fig. 8 Plot of mean of $i(t)$, obtained from 100 simulation runs of (8) and (12) for parametric values $\alpha_0 = 1.305 \times 10^6$, $\beta_0 = 3.858 \times 10^{11}$, $\zeta_0 = 11.58$, $\eta_0 = 4{,}728{,}230$ and fixed forcing intensities $\sigma_1 = 6.43 \times 10^4$, $\sigma_2 = 3.59 \times 10^{10}$, $\sigma_3 = 0.015$ and $\sigma_4 = 3.82 \times 10^5$

In the present work, the stochastic approach has been successfully implemented in analyzing the flow of current through a living cell in the presence of micro-organelles and charged biomolecules. We are in a position to make an attempt to interpret our results from

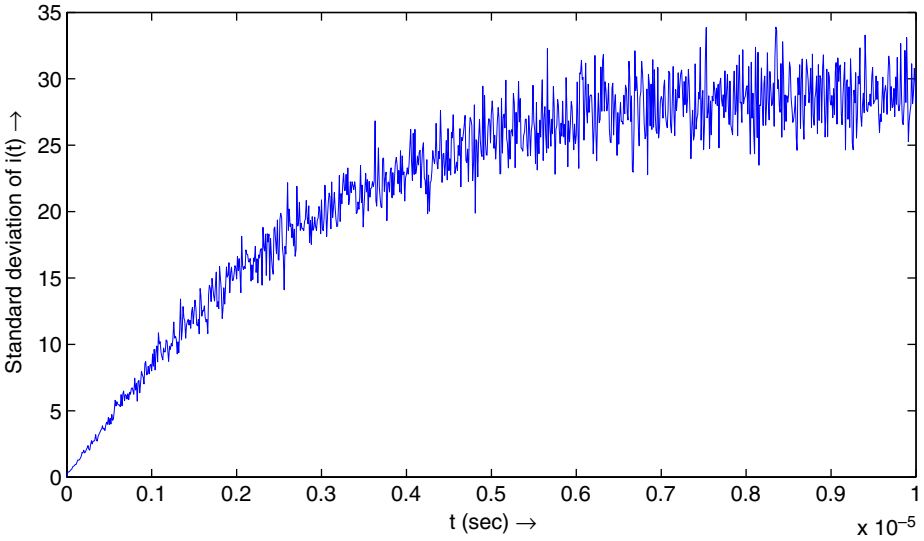

Fig. 9 Plot of standard deviation of $i(t)$, obtained from 100 simulation runs of (8) and (12) for parametric values as mentioned in the caption of Fig. 7

the perspectives of the biophysical aspects of the problem. One of the important results is that the stochasticity in the nuclear membrane capacitance has the most significant effect on the time constant evolution. From fundamental physics, it is known that capacitance is equal to the total charge at a given potential difference. From the biological point of view, the unique structure of the nuclear membrane of any eukaryotic cell is characterized by the presence of nuclear pore complexes contained within the inner and outer nuclear membranes [10]. While the outer nuclear membrane is continuous with the membrane of endoplasmic reticulum, the inner nuclear membrane contains specific proteins (charged entities), which act as binding sites for the nuclear lamina. This entire structure of the nuclear membrane is known as the nuclear envelope. It is known that bi-directional traffic occurs continuously between the cytoplasm and the nucleus through the nuclear pore complexes, which are contained in the nuclear envelope. Such transport of proteins of different sizes and numbers either by free diffusion or by active transport is expected to occur more randomly under the influence of an external electric field. This will lead to more dynamic changes in the total charge difference across the nuclear envelope.

In addition, cell size changes dynamically during the adaptation process of a cell in contact with a biomaterial surface and this occurs with corresponding changes in nuclear size and shape. Under the influence of the electric field, such a phenomenon should be enhanced and this will lead to more random changes in the size of the nucleus. On the basis of the above considerations, it should therefore be realized that random changes in the total charge as well as the area of the nuclear envelope would contribute to the corresponding dynamic changes in C_n, which rationalize an increase in the time constant with an increase in noise in the C_n value.

5 Conclusion

In closing, in order to capture the variability of capacitance and resistance of biological organelles due to fluctuation of cell sizes, we have adopted a stochastic approach to model this realistic phenomenon. The analytical findings along with their validation through numerical simulation were obtained with the help of data from the literature for physical properties of cell and nuclear membranes.

In summary, the stochastic approach has been successfully implemented in analyzing the flow of current through a living cell, considering the randomness of biological interactions with external field. The presented stochastic model clearly reveals that the noise in nuclear membrane capacitance (C_n) is the determining factor as far as the interaction of E-field with a biological cell is concerned and the analytical approach enables in capturing a more realistic estimation of the fluctuating nature of the time constant. For different forcing intensities, the bandwidth of the current through biological cells with advancement of time changes. However, they fluctuate around some average value i.e. the steady state value obtained from the deterministic model. The magnitude of the current at a time equal to the time constant also varies in different runs of numerical simulations, essentially reflecting the stochastic characteristics of the studied biological phenomenon. The analytical results have been rationalized on the basis of biological structure and the dynamic physical process of protein transport through the nuclear membrane.

Acknowledgements The authors thank Department of Science and Technology, India, for financial support. The authors are thankful to the anonymous reviewer for constructive suggestions.

References

1. Dini, L., Abbro, L.: Bioeffects of moderate-intensity static magnetic fields on cell cultures. Micron **36**, 195–217 (2005)
2. Short, W.O., Goodwill, L., Taylor, C.W., Job, C., Arthur, M.E., Cress, A.E.: Alteration of human tumor cell adhesion by high strength static magnetic field. Invest. Radiol. **27**, 836–840 (1992)
3. Ottani, V., Raspanti, M., Martini, D., Tretola, G., Ruggeri, Jr., A., Franchi, M., Piccari, G.G., Ruggeri, A.: Electromagnetic stimulation on the bone growth using backscattered electron imaging. Micron **33**, 121–125 (2002)
4. Panagopoulos, D.J., Messini, N., Karabarbounis, A., Filippetis, A.L., Margaritis, L.H.: A mechanism for action of oscillating electric fields on cells. Biochem. Biophys. Res. Commun. **272**, 634–640 (2000)
5. Kirson, E.D., Gurvich, Z., Schneiderman, R., Dekel, E., Itzhaki, A., Wasserman, Y., Schatzberger, R., Palti, Y.: Disruption of cancer cell replication by alternating electric fields. Cancer Res. **64**, 3288–3295 (2004)
6. Panagopoulos, D.J., Karabarbounis, A., Margaritis, L.H.: Mechanism for action of electromagnetic fields on cells. Biochem. Biophys. Res. Commun. **298**, 95–102 (2002)
7. Basset, C.A.: The development and application of pulsed electromagnetic fields for ununited fractures and arthrodeses. Clin. Plast. Surg. **12**, 259–277 (1985)
8. Joshi, R.P., Hu, Q., Aly, R., Schoenbach: Self-consistent simulations of electroporation dynamics in biological cells subjected to ultrashort electrical pulses. Phys. Rev. E **64**, 259–277 (1985)
9. Dubey, A.K., Gupta, S.D., Kumar, R., Tewari, A., Basu, B.: Time constant determination for electrical equivalent of biological cells. J. Appl. Phys. **105**, 084705 (2009)
10. Ratner, B., Hoffman, A.S., Schoen, F.J., Lemons, J.E.: Biomaterials Science: An Introduction to Materials in Medicine. Academic Press, San Diego (1996)
11. Saha T., Bandyopadhyay, M.: Dynamical analysis of a delayed ratio-dependent prey predator model within fluctuating environment. Appl. Math. Comput. **196**, 458–478 (2008)
12. Bandyopadhyay, M., Chakrabarti, C.G.: Deterministic and stochastic analysis of a non-linear prey-predator system. J. Biol. Syst. **11**, 161–172 (2003)
13. Bandyopadhyay, M., Chattopadhyay, J.: Ratio-dependent predator-prey model: effect of environmental fluctuation and stability. Nonlinearity **18**, 913–936 (2005)
14. Bandyopadhyay, M., Saha T., Pal, R.: Deterministic and stochastic analysis of a delayed allelopathic phytoplankton model within fluctuating environment. Nonlinear Anal. Hybrid Syst. **2**, 958–970 (2008)
15. Gardiner, C.M.: Handbook of Stochastic Methods for Physics, Chemistry and the Natural Sciences. Springer, New York (1985)
16. Horsthemke, W., Lefever, R.: Noise Induced Transitions: Theory and Applications in Physics, Chemistry and Biology. Springer, Berlin (1984)
17. Arnold, L.: Stochastic Differential Equations: Theory and Applications. Wiley, New York (1974)
18. Mao, X.: Stochastic Differential Equations and Applications. Horwood Publishing, England (1997)
19. Oksendal, B.K.: Stochastic Differential Equations: An Introduction with Applications. Springer, New York (2003)
20. Gard, T.C.: Introduction to Stochastic Differential Equations. Marcel Dekker, New York (1988)
21. Kloeden, P.E., Platen, E.: Numerical Solution of Stochastic Differential Equations. Springer, Berlin (1995)